Eur. Phys. J. B **10**, 257–262 (1999)

THE EUROPEAN PHYSICAL JOURNAL B

EDP Sciences

Charge confinement effect in cuprate superconductors: an explanation for the normal-state resistivity and pseudogap

C.C. Tsuei[a] and T. Doderer

IBM Thomas J. Watson Research Center, PO Box 218, Yorktown Heights, NY 10598, USA

Received 7 December 1998

Abstract. The fact that the stripe phase and pseudogap in the cuprate superconductors occur in the same doping regime is emphasized. A model based on charge confinement in self-organized nanometer-scale stripe fragments is proposed to understand various generic features of the normal-state energy gap including the magnitude of the gap, its anti-correlation with the superconducting gap, and the d-wave symmetry in its **k**-dependence. This model also provides a basis for understanding other anomalous normal-state properties such as the linear temperature dependence of electrical resistivity.

PACS. 74.25.-q General properties; correlations between physical properties in normal and superconducting states – 74.25.Fy Transport properties (electric and thermal conductivity, thermoelectric effects, etc.) – 71.10.Li Excited states and pairing interactions in model systems

1 Introduction

After more than ten years of extensive research on superconductivity in cuprates, it is generally agreed that the normal-state of the high-temperature superconductors is significantly different from that of their low temperature conventional counterparts. It has also become increasingly clear that an understanding of the normal state is a prerequisite to the eventual resolution of the mechanism responsible for high-temperature superconductivity. Among the most intriguing normal-state properties are the linear temperature-dependent resistivity, pseudogap phenomena, and the stripe phase. In this work, we will show that they are closely related. Based on charge confinement in nanometer-scale stripe fragments, we will present a model to explain the pseudogap and the linear temperature-dependent resistivity as a function of doping.

The normal-to-superconducting phase transition temperature (T_c) marks the inception of a macroscopic phase-coherent pair state. The existence of a superconducting gap, Δ_S, is well-established by numerous experiments [1]. In the conventional low-T_c s-wave superconductors such as Al, Hg, Pb, etc., a gap is found over the entire Fermi surface. In the high-T_c cuprate superconductors, recent phase-sensitive pairing symmetry tests [2,3] have concluded that the wave vector (**k**) dependent order parameter $\Delta_S(\mathbf{k})$ is a complex number with d-wave symmetry. In other words, the gap $\Delta_S(\mathbf{k})$ varies as $k_x^2 - k_y^2$ and changes its sign across the node lines $k_x = \pm k_y$. While the almost decade-long intense debate on the symmetry of the superconducting gap draws to an end, another gap, also with d-wave symmetry, is found recently in the normal state of many cuprate superconductors [4–7]. This normal-state energy gap (Δ_N), also called pseudogap, is characterized by a depression in the electronic excitation spectrum. The quasiparticle density of states is reduced but does not vanish in any direction unlike in the case of a d-wave superconducting gap. The experiments [8–10] that have suggested the existence of a pseudogap include: NMR, Raman spectroscopy, neutron scattering, measurements of electrical resistivity, Hall effect, thermopower, optical conductivity, specific heat, and angle-resolved photoemission spectroscopy (ARPES). In particular, several recent high-resolution ARPES experiments [4–7] have convincingly shown that the pseudogap opens at a temperature T^* well-above T_c, and has the identical characteristic **k**-dependence in amplitude as that of the d-wave superconducting gap Δ_S. From the analysis of the ARPES, heat capacity and magnetic susceptibility data, it is concluded [8,10] that the observed pseudogap is from charge excitation and there is no separate spin gap. The normal-state gap has been observed mostly in the under-doped region and it vanishes gradually at or near the optimal doping. There is apparently no theoretical model that can describe satisfactorily all the generic features associated with the pseudogap.

Another interesting and equally intriguing phenomenon discovered in the same doping range of the cuprate superconductors is the formation of the stripe phase [11–13]. It is a manifestation of temporal and spatial modulations of charges (dopant-induced holes) and the spins associated with the copper atoms in the CuO_2 planes. Based on the results of neutron scattering experiments by Tranquada *et al.* [11], it is concluded

[a] e-mail: tsuei@watson.ibm.com

that the in-plane holes segregate into periodically-spaced stripes between the intervening anti-ferromagnetic insulating/semiconducting domains with periodicity different from that of the underlying crystal lattice. The incommensurate periods of the charge stripes and the spin-spin correlation length are of the order of nanometers, and are doping dependent. The fact that similar topological stripe phases were also found in nickelates and manganites suggests that it may be a common feature of strongly correlated electron systems. There have been several theoretical models studying the origin of the stripe phase [14–16]. In this work, we will not deal with this issue. Rather, we will utilize the experimental fact that the periodic charge and spin modulations are on the scale of nanometers. The energy levels of the charges confined in such small volumes are quantized just as in the case of quantum dots [17]. This charge confinement effect together with quantum fluctuations of the order parameter ($\Delta_{\rm S}$) in these nanometer-scale grains offer a natural explanation for the pseudogap phenomena. Our charge confinement model also provides a basis for understanding various anomalous normal-state properties of the cuprates, including the linear temperature dependence of resistivity.

The neutron scattering experiments have convincingly established the existence of stripe phase in various oxides [11,12]. In cuprates such as $La_{2-x}Sr_xCuO_4$ (LSCO) and $YBa_2Cu_3O_{7-y}$ (YBCO), the charge and spin modulations fluctuate with time and position. The stripes can be static through impurity pinning as demonstrated in the Nd-doped LSCO [11]. Actually, alternating metallic (charge-rich) and semiconducting (charge-poor) stripes with nanometer dimensions were observed [18] as early as 1989 in the local conductance images of YBCO crystals with a high-resolution cross-sectional scanning tunneling microscope (STM). On the surface of the *in situ*-cleaved YBCO crystals the stripes are pinned by certain surface features. The surface of the YBCO crystals probed by STM may be under-doped because of the escape of the oxygen into the vacuum. The results of the STM experiments [18] indicate that the stripes are fractured into pieces with a length of about 50 to 100 Å which is about four times the spin-spin correlation length as deduced from the neutron scattering data [11]. The STM results also suggest that the height of the stripes is equal to one c-axis lattice constant (c = 11.7 Å for YBCO). Recent observations [19,20] of electronic modulations along the Cu–O chains in YBCO are consistent with our STM observation of stripe fragmentation [18]. Furthermore, recent electron microscopy studies on perovskite manganites [21] also indicate that the existence of stripe fragmentation is probably a general feature of strongly electron correlated oxide systems. The in-plane period of the stripes in cuprates near the optimal doping, as suggested from the neutron scattering data, is about 15 Å for LSCO and YBCO. Based on the STM and the neutron scattering data, one can envision that the holes reside in nanometer-scale boxes with an average dimension of $15 \times 13 \times 60$ Å^3 in LSCO, for instance. The charge boxes are separated by insulating/semiconducting antiferromagnetic domains of similar sizes. In the following, we will propose a model, based on quantization effects arising from the charge confinement in these nano-boxes, to understand the pseudogap phenomena in cuprate superconductors. In particular, we will look for an energy scale and its doping dependence corresponding to T^* and its anti-correlation with $T_{\rm c}$ in the under-doped regime.

2 Normal-state resistivity

Before this is done, we will test the idea of quasi-1D charge boxes by considering the temperature and doping dependences of the in-plane resistivity. Extensive studies [9,22–24] on normal-state resistivity $\rho(T)$ in various cuprate superconductors in the optimal and under-doped regimes have firmly established the following universal behavior: 1) a linear temperature-dependent resistivity that shows no saturation up to a temperature as high as 1000 K (for example, see the $\rho(T)$ data of the LSCO system in Fig. 1); 2) an identical value of the temperature coefficient $\mathrm{d}\rho/\mathrm{d}T$ (1.2 $\mu\Omega$cm/K) to within 20% for many cuprates at optimal doping [25]. For a given cuprate system such as the LSCO superconductors, the slope $\mathrm{d}\rho/\mathrm{d}T$ increases with decreasing doping (see the inset of Fig. 1). The linear-T dependence of resistivity is deviated below T^* which signals the opening of a pseudogap. In the under-doped regimes, the sharp rise in $\rho(T)$ below the shallow resistivity minimum (Fig. 1) has been attributed to hopping conductivity of localized charge carriers [24].

To understand the linear-T resistivity phenomena, we recall the exact theorems that state that all electronic states in any disordered one-dimensional structure are localized [26]. Electronic conduction based on phonon-induced hopping and diffusing processes involving such localized states has been established for more than thirty solids [27]. At low temperatures, charge transport is dominated by the well-established process of hopping conduction. At high enough temperatures, however, the conduction is mainly diffusive. The temperature-dependent resistivity, $\rho(T)$, due to charge diffusion is always linear in temperature (in the high temperature limit ($T > T^*$) where the thermal energy is much larger than the potential barrier for the localized states inside the grains) and can be described by the well-known Einstein formula:

$$\rho(T) = \left(\frac{k_{\rm B}T}{ne^2}\right) \frac{d}{\langle\nu_0\rangle\langle(\mathbf{r}_i - \mathbf{r}_j)^2\rangle} \qquad (1)$$

where n is the charge-carrier concentration, d the dimensionality, $\langle\nu_0\rangle$ average carrier jumping frequency, and $\langle(\mathbf{r}_i - \mathbf{r}_j)^2\rangle$ average phonon-assisted electronic random-walk distance squared involving states centered on $\mathbf{r}_i$ and $\mathbf{r}_j$ [27]. The quantity $\langle\nu_0\rangle\langle(\mathbf{r}_i - \mathbf{r}_j)^2\rangle/d$ is the diffusion constant $D(d)$. In the case of a cuprate superconductor, if the charge transport is mostly *via* the conduction through the stripes, then $d = 1$ in equation (1). The quantity n is the product of the number of charge stripes per cross-sectional area and the charge density per unit length of the stripe. Therefore, n is proportional to the number of

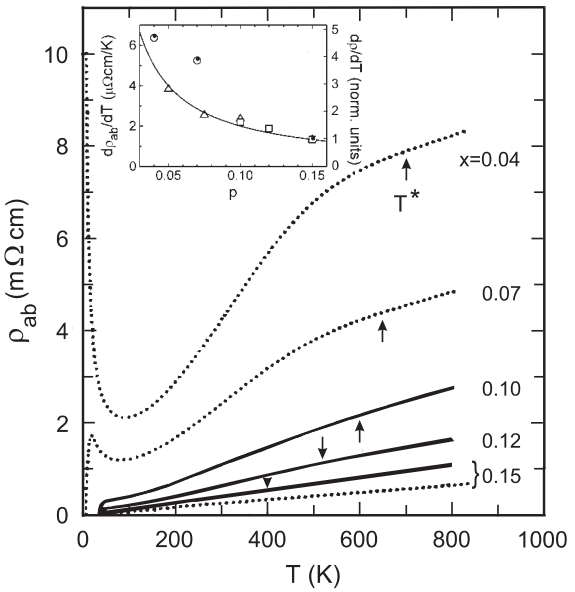

Fig. 1. In-plane resistivity $\rho_{ab}(T)$ as a function of temperature for $La_{2-x}Sr_xCuO_4$ with various doping concentrations, $x \approx p$ (after Refs [22,23] where p is the number of holes per CuO_2 plane. The dotted and solid curves are for the epitaxial films [22] and single crystals [23] respectively. The arrows mark the opening of the pseudogap T^*. In the inset, the $d\rho_{ab}/dT$ data are plotted as a function of p: ($\odot$) c-axis oriented epitaxial films [22]; ($\triangle$) polycrystals [22]; and ($\square$) single crystals [23]. All three sets of data are presented in units normalized at the optimal doping ($p = 0.15$) to remove any uncertainty arising from the sample geometrical configuration. The values of $d\rho/dT$ at $p = 0.15$ are: 0.76 (epitaxial films); 3.82 (polycrystals) and 1.33 (single crystals) in the units of $\mu\Omega$cm/K. The $d\rho_{ab}/dT$ results for the single crystals are also shown in the absolute units (left vertical axis) in the inset. The solid curve is the prediction of equation (1) on the doping dependence of $d\rho/dT \propto 1/p$, as discussed in the text.

holes (p) per Cu in the CuO_2 planes (for example, $x \approx p$ in the $La_{2-x}Sr_xCuO_4$ system). As indicated by equation (1), the diffusive charge conduction is always characterized by a linear temperature dependence of resistivity, irrespective of the dimensionality d. To show that low-dimensional charge transport indeed prevails in the normal-state of the cuprates, we first examine the in-plane resistivities (ρ_a and ρ_b, a and b refer to the crystallographic axes) as a function of temperature in an untwinned and optimum oxygenated YBCO single crystal [28]. In terms of our stripe-based charge-diffusion model and equation (1), we expect the following: 1) both $\rho_a(T)$ and $\rho_b(T)$ depend linearly on temperature; 2) $\rho_a(T) > \rho_b(T)$, if the stripes are running in the b direction; 3) as temperature increases to a crossover point (T_D) when the diffusion length ℓ_D is about equal to the stripe width (~ 15 Å), $d\rho_b/dT$ should change gradually by a factor of two. This signifies the 1D to 2D dimensional crossover based on equation (1) (*i.e.* the value of d changes from 1 to 2); and 4) for $T > T_D$, $d\rho_a/dT$ and $d\rho_b/dT$ are equal because the charge transport in the direction perpendicular to the stripe direction b is always 2D in nature. All the above predictions were indeed observed [28]: $d\rho_a/dT = 1.16$ $\mu\Omega$cm/K; for $\rho_b(T)$ a change of the temperature coefficient was observed at $T_D \approx 270$ K and $d\rho_b/dT = 0.52$ $\mu\Omega$cm/K for $T < T_D$ and $d\rho_b/dT = 1.08$ $\mu\Omega$cm/K for $T > T_D$. The fact that $d\rho_b/dT$ increases precisely by a factor of two above T_D represents a strong supporting evidence for the stripe model. The crossover diffusion length can be estimated by using the following formula: $\ell_D = \sqrt{\hbar D/(k_B T_D)}$. The value of D can be calculated from the experimental values of $d\rho/dT$ and the equation (1) for a given doping concentration p and dimensionality. For YBCO at optimal doping ($p = 0.15$), ℓ_D is found to be about 14 Å for $T_D = 270$ K, $D = 6.5 \times 10^{-5}$ m^{2}s^{-1} which corresponds to $d\rho_b/dT = 0.52$ $\mu\Omega$cm/K. This value is very close to the stripe period (~ 15 Å) deduced from the neutron scattering experiment [11]. As a second example, we will use our stripe model to understand $d\rho_{ab}/dT$ as a function of doping (p) in the LSCO system. Since the widths of the stripes in YBCO and LSCO are about the same, $\rho(T)$ is in the 2D regime and there should be no dimensional crossover in the temperature range of $T > T^* > T_D$ (≈ 300 K). This is indeed consistent with the results of many resistivity measurements (see, for example, Fig. 1). Furthermore, the fact that the magnitude of $d\rho_{ab}/dT$ in single crystal LSCO (~ 1.3 $\mu\Omega$cm/K) is about the same as that of $d\rho_a/dT$ or $d\rho_b/dT$ of YBCO in the 2D regime suggests that the optimum-T_c cuprate superconductors are characterized by a universal $d\rho/dT$ of ~ 1 $\mu\Omega$cm/K at high temperatures ($T > T^*$) in good agreement with the experiments [25]. In terms of the equation (1), this implies that the diffusion constant $D(2)$ is approximately constant and is not strongly doping dependent. Based on these considerations, equation (1) predicts that $d\rho/dT$ should be inversely proportional to the hole concentration p. This is in good agreement with three sets of data available in the literature for the LSCO system (see the inset in Fig. 1).

3 The model

In the study of pseudogap, the relevant energy scale will be set by the length of the stripe fragments (L) which can be estimated by the temperature T_H at which the diffusive charge transport inside the fragments ceases to be effective, when the thermal diffusion length ℓ_H is larger than L, and is replaced by ballistic conduction. The overall conduction is then dominated by variable range hopping ($T < T_H$). The length ℓ_H is related to T_H by the diffusion formula: $\ell_H = \sqrt{\hbar D/(k_B T_H)}$ used before. As an example, T_H is approximately 100 K for $p = 0.04$ (see Fig. 1 and also data in Ref. [24]). This leads to $\ell_H \approx 20$ Å. The doping dependence of T_H in LSCO system has been studied by Ellman *et al.* [24]. Based on these results one concludes that ℓ_H increases with increasing doping. These results support that the length of the charge boxes is indeed of the order of 20–100 Å and are in agreement with the STM results [18]. In addition, a recent theoretical calculation by White and Scalapino based on the 2D t-J model also indicates

the existence of charge-poor and charge-rich regions ($\sim$ 80 Å) along the stripes [29]. A similar conclusion on the width of stripes in LSCO system as a function of doping has been obtained by a recent neutron scattering experiment [30]. As a first approximation, in this study we assume that the width and the length of the stripes decrease linearly with decreasing doping concentration. The height (= 13.3 Å) remains a constant of doping. Since the time scale of the stripe fluctuation is of the order of a few ps [16] and thus two orders of magnitude slower than the transit time of the charge carriers through the stripe fragments ($\approx$ 10 fs) (estimated from the stripe length and the Fermi velocity), we therefore assume a static stripe phase for our calculations.

Inspired by the recent elegant superconductivity experiments [31] on nanometer-scale Al particles, the very definition of superconductivity in ultrasmall particles are re-examined in terms of the even-odd parity effect and quantum fluctuations [32–34]. To study the ground state energies of small superconducting grains, Matveev and Larkin (ML) [32] use following pairing Hamiltonian:

$$H = \sum_{j\sigma} \epsilon_j a^\dagger_{j\sigma} a_{j\sigma} - g \sum_{jj'} a^\dagger_{j\uparrow} a^\dagger_{j\downarrow} a_{j'\downarrow} a_{j'\uparrow} \qquad (2)$$

where ϵ_j is the single particle energy level and the average level spacing is defined as $\delta_\epsilon = \langle \epsilon_{j+1} - \epsilon_j \rangle$. The operator $a^\dagger_{j\sigma}$ creates a charge state with quantum number j and spin σ, and g is the pairing interaction strength. The work by ML clearly shows that in the small grain limit ($\delta_\epsilon \gg \Delta_S$), quantum fluctuations induced corrections to the standard BCS mean-field approximation become important. As the grain size decreases, the small grain system described by equation (2) exhibits a superconducting to normal crossover that is dominated by the fluctuations of the order parameter Δ_S, the BCS superconducting gap. The physics of quantum fluctuations can be traced back to the effect of logarithmic renormalization [32]. This effect is not predicted by the BCS mean-field approximations. As a result of quantum fluctuations, the energy correlations are short-ranged in the normal state [33]. Based on the same Hamiltonian (2), Mastellone, Falci, and Fazio (MFF) [33] studied pair correlations in ultrasmall grains in the canonical ensemble. The results of this numerical calculation confirm the analytic results of ML on the ground state energy in the small and large grain limits. Furthermore, they computed the spectroscopic gap E_G, the energy that separates the ground state and the first excited many-body level. They demonstrated that both the ground state energy and E_G are parity-dependent and are universal functions of δ_ϵ/Δ_S.

In the present work, we have identified the spectroscopic gap as the energy scale in the pseudogap problem of cuprate superconductors (*i.e.* $E_G = ak_BT^* = \Delta_N$, $a \approx 1$). We will concentrate on the LSCO system for the reason that some data on doping dependence of the stripe phase are available as discussed earlier. From the previous discussion, we have concluded that the average size of the fragments of the stripes in LSCO near the T_c-optimal compositions is about 15 Å $\times$ 13.3 Å (c-axis lattice constant) $\times$ 60 Å. The exact charge distribution in such nanograins is not experimentally determined but is believed to reflect the balance between charge-charge correlation and hybridization. As a function of decreasing doping, the holes tend to localize to form one-dimensional sheets. In the absence of experimental data on the doping dependence of the charge distribution, we will assume that the holes are uniformly distributed in the charge boxes except at the composition range where x is less than about 0.05. We can now proceed to calculate the number of holes in the charge box, N. For LSCO, N is found to be 83 for $p = 0.2$ (nanograins with an average volume of $20 \times 13 \times 75$ Å^3). The quantum level spacing δ_ϵ can be estimated by:

$$\delta_\epsilon \approx \frac{2\pi^2\hbar^2}{3m^*V^{2/3}N^{1/3}} \qquad (3)$$

where m^* is the effective mass of the charge, and V is the volume of the box. For the present study, we assume m^* is equal to the free electron mass in the nanobox. For $N = 83$, $\delta_\epsilon \approx 15$ meV. We are ready to apply the MFF numerical results to determine E_G. We first determine Δ_S for a given hole concentration p by making use of the following empirical formula for T_c [8,10] and Δ_S:

$$\frac{T_c}{T_{c,\max}} = 1 - 82.6(p - 0.16)^2 \qquad (4)$$

where $T_{c,\max} = 38$ K for LSCO and $\Delta_S = 2.5\,k_BT_c$. The numerical data of MFF on E_G/δ_ϵ which is a universal function of δ_ϵ/Δ_S, can then be used to determine the value of E_G as a function of doping. For example, the ratio $\delta_\epsilon/\Delta_S \approx 2$ (for $p = 0.2$) leads to the following results: $E_G = 13.5$ meV for odd-number grains, and $E_G = 24.5$ meV for even-number grains. As expected, the lowest energy needed to excite an even-number particle is higher than that for an odd-number counterpart which already has an unpaired charge. A bulk sample may consist of charge stripe fragments with both even and odd number of charges. The exact even–odd ratio is not known. Furthermore, the length of the fractured stripes may vary. It should be pointed out that extra long stripes are probably not stable against fragmentation. The stripes with a much below-average length will give rise to an E_G much higher than the average value [35]. Another factor that should be taken into account is that in the case of d-wave superconductors, the parity effect is reduced by a factor of $\sqrt{N}$, as pointed out by Golubev and Zaikin [34] recently. This effect is most pronounced near the optimal compositions and gradually diminishes in the low doping region. Because there is already an unpaired charge in the odd-number grains, the d-wave correction is most pronounced in the even-number grains. Therefore we assume that the value of E_G in the odd-number grains remains unchanged by this effect in our calculation. For example, in the case of $p = 0.2$, the corrected values of E_G are 15 meV (13.5 meV) for the even (odd) grains.

With the above considerations in mind, we present our calculated values of E_G as a function of doping p in Figure 2. For comparison, the experimental data of T^* obtained with various charge- and spin-response probes are

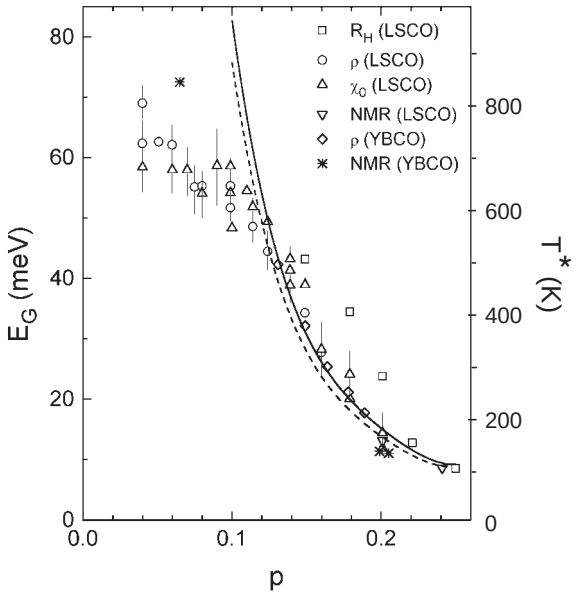

Fig. 2. A comparison between the experimental T^* data (after Refs [8–10]) and the calculated values of the excitation gap E_G as a function of doping p for the $La_{2-x}Sr_xCuO_4$ (LSCO) system. The solid and dashed curves are for even and odd-number systems respectively. The experimental results are compiled from various spin- and charge-response measurements as indicated by different symbols in the figure legend. Some of the YBCO data are also included to demonstrate the universality of the pseudogap phenomena. A preliminary calculation of E_G for YBCO (assuming the same size for the nanograins) indicates a slight change of 10–20% from those calculated for LSCO, still well within the scatter of the experimental data.

plotted in the same figure. As shown in Figure 2, the calculated results have definitely provided an energy scale that corresponds to the pseudogap data k_BT^*. The doping dependence of T^* can be understood fairly well except in the low doping regime. It is possible that the nanograin system crosses over to the regime of one-dimensional charge confinement, and the formula for the δ_ϵ estimate is no longer valid. Also, if the charge and spin stripes are not equal in width, the effective doping per grain increases resulting in a decrease of δ_ϵ. Furthermore, the issue of sample inhomogeneity may become more acute in this low doping region.

4 Discussion

As seen in Figure 2, the results of our calculations based on charge confinement in nanograins have captured the essential features of the pseudogap in cuprate superconductors. Our model provides not only the correct energy scale for T^*, it also explains why the magnitude of the normal-state energy gap anti-correlates with the size of the superconducting gap (*i.e.* T_c), and why the pseudogap gradually disappears in the over-doped regime. The fact that both E_G and Δ_S are determined by the same underlying pairing interaction (*i.e.* the same Hamiltonian, Eq. (2)) guarantees that they will have the same **k**-dependence. This gives a natural explanation for the d-wave symmetry observed for both the normal-state [5,6] and superconducting gaps [3] in $Bi_2Sr_2CaCu_2O_{8+y}$. Although this conclusion requires no knowledge of the microscopic mechanism for the pairing interaction (g in Eq. (2)). It is of interest to note that the nano-scale charge-stripe fragments discussed here represent a close analogy of quantum dots [17]. Electrons or holes confined in a nanometer-scale grain can enhance charge-charge correlations that could lead to attractive interaction [17]. In fact, BCS pairing induced excitation gap (parity gap) in nuclei due to particle confinement was suggested [36] in 1958 soon after the advent of the BCS theory of superconductivity.

In the same doping range where the pseudogap is observed, there are also many anomalous properties above T_c in the cuprate superconductors that are considered to be the signatures of a non-Fermi liquid normal state. It may be worthwhile to re-consider these unusual characteristics of cuprates in the light of a model based on alternating hole-rich and hole-poor nanograins. The quasi-1D nature of the charge boxes makes the conventional electron-phonon scattering process ineffective for charge transport due to limitations of available phase space. This is consistent with the fact that the linear temperature dependence of resistivity cannot be understood in terms of standard electron-phonon scattering mechanism. On the other hand, the 1D nature of charge transport inherent in the stripe phase results in a forward scattering process which may favor the occurrence of high-T_c superconductivity in cuprates [37]. In addition to the evidence presented in this work, another strong evidence for quasi 1D electronic structure in YBCO-systems is the ARPES observation of extended (1D) Van Hove singularity along the Γ-Y direction [38], which is parallel to the Cu–O chains (stripes). The Van Hove singularity has been discussed in the literature as a possible T_c-enhancement mechanism [39].

As another example, the two relaxation rates observed [40] in the LSCO system may just be a manifestation of the different scattering times in the charge stripes and the in-between antiferromagnetic domains. The discreteness of the energy levels in the box should manifest itself in the quasiparticle tunneling spectroscopy of the metallic (charge-rich) stripes but not the insulating (charge-poor) stripes. This apparently has been observed in an STM experiment [18] with YBCO. A recent observation [41] of a low-temperature pseudogap in the vortex cores of $Bi_2Sr_2CaCu_2O_{8+y}$ can be understood in the sense that the vortex core is in the normal-state albeit at a temperature below T_c. More interestingly, the observed unusually large doping-dependent energy gap (Δ_p) in $Bi_2Sr_2CaCu_2O_{8+y}$ [41,42] can be quantitatively identified with the spectroscopic gap E_G in our model. Therefore, the smooth variation of Δ_p across T_c, as observed in spectroscopic measurements [41,42] finds a natural explanation now.

Our calculation of E_G makes use of the numerical results based on an isolated superconducting grain with a fixed number of particles [33]. In realistic samples, there must be coupling between the nanograins *via* particle

exchange. As a consequence, an itinerant particle will choose to reside in an odd-number grain for energetic reasons (the pairing energy g is gained and the cost of E_G is avoided). Therefore, in equilibrium, the even-number grains outnumber the odd ones, resulting in a reduced spin susceptibility in the pseudogap state as observed experimentally [8,9]. The fact that the experimental data for T^* can be well-described by the calculated E_G suggests that this coupling is not large enough to smear out the discrete quantum level effect at least for $T < T^*$. In fact, intergrain particle exchange (*i.e.* the fixed particle number assumption is relaxed) allows a macroscopic phase-coherent superconducting state to establish below T_c. This interaction can be accomplished by the Josephson coupling between the grains, for instance. Indeed, the hysteretic magnetic susceptibility as a function of field and temperature in cuprate superconductors was explained in terms of a spin-glass-model [43]. This model is based on a 2D disordered array of Josephson coupled domains of about 100 Å in size. An estimate for the in-plane critical current density J_c based on this array of nanometer-scale Josephson junctions yields $J_c \approx 8 \times 10^7$ A/cm^2 at low temperature, assuming that the Josephson coupling energy $E_J = \hbar I_c/(2e) = k_B T_c$ ($T_c = 100$ K), where I_c is the intergrain critical current. A recent analysis of the temperature dependence of J_c also suggests Josephson-coupled domains in various YBCO samples [44].

We would like to thank M.B. Ketchen, R.H. Koch, D. Mitzi, I. Morgenstern, D.M. Newns, P.C. Pattnaik, Ch. Renner, J.Z. Sun and J.M. Tranquada for useful discussions.

References

1. M. Tinkham, *Introduction to Superconductivity*, 2nd edition (McGraw-Hill, New York, 1996).
2. C.C. Tsuei *et al.*, Phys. Rev. Lett. **73**, 593 (1994).
3. C.C. Tsuei, J.R. Kirtley, Physica C **282–287**, 4 (1997) and the references therein.
4. A.G. Loeser, Z.-X. Shen, D.S. Dessau, D.S. Marshall, C.H. Park, P. Fournier, A. Kapitulnik, Science **273**, 325 (1996).
5. H. Ding, T. Yokaya, J.C. Campuzano, T. Takahashi, M. Randeria, M.R. Norman, T. Mochiku, K. Kadowaki, J. Giapinzakis, Nature **382**, 51 (1996).
6. Z.-X. Shen *et al.*, Science **280**, 259 (1998).
7. N.L. Saini, J. Avila, A. Bianconi, A. Lanzara, M.C. Asensio, S. Tajima, G.D. Gu, N. Koshizuka, Phys. Rev. Lett. **79**, 3467 (1997).
8. J.R. Cooper, J.W. Loram, J. Phys. I France **6**, 2237 (1996).
9. B. Batlogg *et al.*, Physica C **235–240**, 130 (1994).
10. G.V.M. Williams *et al.*, Phys. Rev. Lett. **78**, 721 (1997).
11. J.M. Tranquada, Physica C **282–287**, 166 (1997) and the references therein.
12. P. Dai, H.A. Mook, F. Dogan, Phys. Rev. Lett. **80**, 1738 (1998).
13. B. Goss Levi, Physics Today (June 1998), p. 19.
14. J. Zaanen, W. van Saarloos, Physica C **282–287**, 178 (1997).
15. O. Zachar, S.A. Kivelson, V.J. Emery, Phys. Rev. B **57**, 1422 (1998).
16. V.J. Emery, S.A. Kivelson, O. Zachar, Phys. Rev. B **56**, 6120 (1997).
17. R.C. Ashoori, Nature **379**, 413 (1996).
18. C.J. Chen, C.C. Tsuei, Solid State Commun. **71**, 33 (1989).
19. H.L. Edwards, A.L. Barr, J.T. Markert, A.L. de Lozanne, Phys. Rev. Lett. **73**, 1154 (1994).
20. H.L. Edwards, D.J. Derro, A.L. Barr, J.T. Markert, A.L. de Lozanne, Phys. Rev. Lett. **75**, 1387 (1995).
21. S. Mori, C.H. Chen, S.-W. Cheong, Phys. Rev. Lett. **81**, 3972 (1998).
22. H. Takagi *et al.*, Phys. Rev. Lett. **69**, 2975 (1992).
23. Y. Nakamura, S. Uchida, Phys. Rev. B **47**, 8369 (1993).
24. B. Ellman *et. al.*, Phys. Rev. B **39**, 9012 (1989).
25. N.P. Ong, Y.F. Yan, J.M. Harris, in *Charge transport properties of the cuprate superconductors in High-T_c Superconductivity and the C_{60} Family*, edited by S. Feng, H.C. Ren (Gordon and Breach Publishers, 1995), pp. 53–79.
26. R.E. Borland, Proc. Phys. Soc. London **78**, 926 (1961).
27. A.N. Bloch, R.B. Weisman, C.M. Varma, Phys. Rev. Lett. **28**, 753 (1972).
28. R. Gagnon, C. Lupien, L. Taillefer, Phys. Rev. B **50**, 3458 (1994).
29. S.R. White, D.J. Scalapino, Phys. Rev. Lett. **81**, 3227 (1998).
30. K. Yamada *et al.*, Phys. Rev. B **57**, 6165 (1998).
31. C.T. Black, D.C. Ralph, M. Tinkham, Phys. Rev. Lett. **76**, 688 (1996).
32. K.A. Matveev, A.I. Larkin, Phys. Rev. Lett. **78**, 3749 (1997).
33. A. Mastellone, G. Falci, R. Fazio, Phys. Rev. Lett. **80**, 4542 (1998).
34. D.S. Golubev, A.D. Zaikin, Phys. Lett. A **195**, 380 (1994).
35. We wish to emphasize that our stripe fragments model is distinctly different from the previous work by Bianconi *et al.* [45,46], in which the charge confinement along the stripe length was not considered.
36. A. Bohr, B.R. Mottelson, D. Pines, Phys. Rev. **110**, 936 (1958).
37. R. Zeyher, M.L. Kulić, Phys. Rev. B **53**, 2850 (1996).
38. K. Gofron, J.C. Campuzano, A.A. Abrikosov, M. Lindroos, A. Bansil, H. Ding, D. Koelling, B. Dabrowski, Phys. Rev. Lett. **73**, 3302 (1994).
39. R.S. Markiewicz, J. Phys. Chem. Solids **58**, 1179 (1997) and the references therein.
40. H.Y. Hwang *et al.*, Phys. Rev. Lett. **72**, 2636 (1994).
41. Ch. Renner *et al.*, Phys. Rev. Lett. **80**, 3606 (1998).
42. Ch. Renner *et al.*, Phys. Rev. Lett. **80**, 149 (1998).
43. I. Morgenstern, K.A. Müller, J.G. Bednorz, Z. Phys. B **69**, 33 (1987).
44. H. Darhmaoui, J. Jung, Phys. Rev. B **57**, 8009 (1998).
45. A. Bianconi, M. Missori, J. Phys. I France **4**, 361 (1994).
46. A. Perali, A. Bianconi, A. Lanzara, N.L. Saini, Solid State Commun. **100**, 181 (1996).